Tuning Optical and Electronic Properties of Bithiazole Containing Polymers by *N*-Methylation

Jeffrey K. Politis and M. David Curtis*

Department of Chemistry and the Macromolecular Science and Engineering Center, The University of Michigan, Ann Arbor, Michigan 48109-1055

Yi He and Jerzy Kanicki

Department of Electrical Engineering and Computer Science, Display Technology and Maunfacturing Center, University of Michigan, Ann Arbor, Michigan 48109-2108

Received August 5, 1998; Revised Manuscript Received February 4, 1999

ABSTRACT: The N-atoms in two polymers, poly(4,4′-dinonyl-5,5′-bithiazole-2,2′-diyl-*co*-5-*tert*-butylphenylene-1,3-diyl) (PBT) and poly(4,4′-bis(*p*-dodecylphenyl)-2,2′-bithiazole-5,5′diyl) (DBT), have been quaternized by the reaction of the polymer with methyltriflate to give their respective *N*-methylated derivatives, MPBT and MDBT. Quaternization of the ring nitrogen atom lowers the energy levels of both the HOMO and LUMO and, hence, alters those polymer properties which are dependent on these energy levels. Both the absorbance and emission spectra red shift upon methylation, and the electrochemical reduction potential increases by 0.88 V. An increase of up to 8 orders of magnitude was also observed in the conductivity.

Introduction

Conjugated polymers are being used in several device applications, including light-emitting diodes (LEDs)[1−4] and thin-film transistors (TFTs).[5−7] The performance of both devices depends on the charge mobility; however, the electroluminescence efficiency of an LED is highly sensitive to solid-state morphology changes. For example, π-stacking was shown to greatly enhance interchain electron hopping and, thus, increase the charge mobility.[8,9] However, the alignment of the π-systems 3−4 Å apart engcourages the formation of excimers, [10] and excimers have been shown to quench the luminescence efficiency through the loss of energy by nonradiative processes.[10−14] Hence, the properties that enhance the performance of a TFT, such as the formation of π-stacks, are often detrimental to the operation of an LED. Thus, it is necessary to tune each polymer for a specific application.

One method of tuning polymer properties involves making specific structural changes in the polymer, i.e., replacing an alkyl side chain with an alkoxy group to alter electronic properties in polythiophenes and polyphenylenevinylenes (PPVs). An alternative route is the modification of a functional group on the polymer. Examples include the quaternization of the nitrogen in pyridine-containing polymers with an alkyl group[15] or the complexation of metals to a nitrogen in a bithiazole ring.[16] The latter method is potentially more interesting because of the wide variety of materials obtainable from one basic synthetic route. For example, the properties may be changed by using different percentages of *N*-alkylation or different alkylating agents or, in the case of metal complexation, by using different metals. Also, these methods have the potential of being reversible, thus opening the possibility of utilizing these modifications to form sensors.

The synthesis and characterization of a series of n-dopable, bithiazole-containing polymers have been recently reported.[17−21] It was shown that by tailoring the substituent or comonomer, the structural and optical properties could be altered while keeping other properties constant, such as electrochemical behavior. Here, we report that important properties of these polymers, e.g., reduction potential, emission wavelength, conductivity, solubility, etc., can be altered dramatically by alkylation, i.e., quaternizing the ring nitrogen atom.

Experimental Section

Materials. All manipulations and polymerizations were performed under a nitrogen atmosphere using standard Schlenk line techniques unless otherwise stated. Reagents were purchased and used as received unless otherwise stated.

^{1}H NMR spectra were collected on a Bruker AM-360, AM-300, or AM-200 and referenced to the residual proton solvent resonance. UV−vis spectra were collected on a Shimadzu 3101PC with baseline correction. Emission spectra were collected on a Shimadzu 4121 interfaced with a Gateway computer. Cyclic voltammetry (CV) was run using a home-built potentiostat, designed by Wayne Burkhardt, electronics shop, Department of Chemistry, University of Michigan, interfaced to a PC computer with a custom program written by Dr. S. Paras, Department of Chemistry, University of Michigan. The solvent was dry CH_2Cl_2, and the supporting electrolyte was tetrabutylammonium hexafluorophosphate (0.1 M). The reported potentials are vs the ferrocene/ferrocenium (Fc/Fc^+) couple, obtained by adding a crystal of ferrocene to the solution. Two probe conductivity measurements were performed with a Keithley 617 electrometer on polymer films metallized by evaporation of aluminum. Elemental analyses were performed by either Galbraith Laboratories or the University of Michigan Microanalysis Laboratory.

All of the theoretical calculations were conducted on a Cache work station. Extented Hückel calculations were used to model the molecular orbitals. MOPAC, utilizing the PM3 parameters, was used to optimize the geometry. Zindo, with INDO/1 parameters and the configuration interaction set to 9, was used to model the electronic spectrum.

Synthesis of Methylated Poly(4,4′-dinonyl-5,5′-bithiazole-2,2′-diyl-*co*-5-*tert*-butylphenylene-1,3-diyl) (MPBT). A 250 mL Schlenk flask was charged with poly(4,4′-dinonyl-5,5′-bithiazole-2,2′-diyl-*co*-5-*tert*-butylphenylene-1,3-diyl) (PBT)[17,21] (0.50 g, 0.91 mmol based on repeat) in $CHCl_3$ (100 mL). Methyltriflate (1.74 g, 1.2 mL, 10.6 mmol) was added in 0.2 mL increments over 2 days. After 1 day, the solution was heated to 35−40 °C. A solid coated the flask over time. $CHCl_3$

10.1021/ma981242a CCC: $18.00 © 1999 American Chemical Society
Published on Web 04/01/1999

Scheme 1. Synthesis of the Methylated Polymers (50% Methylated Shown)

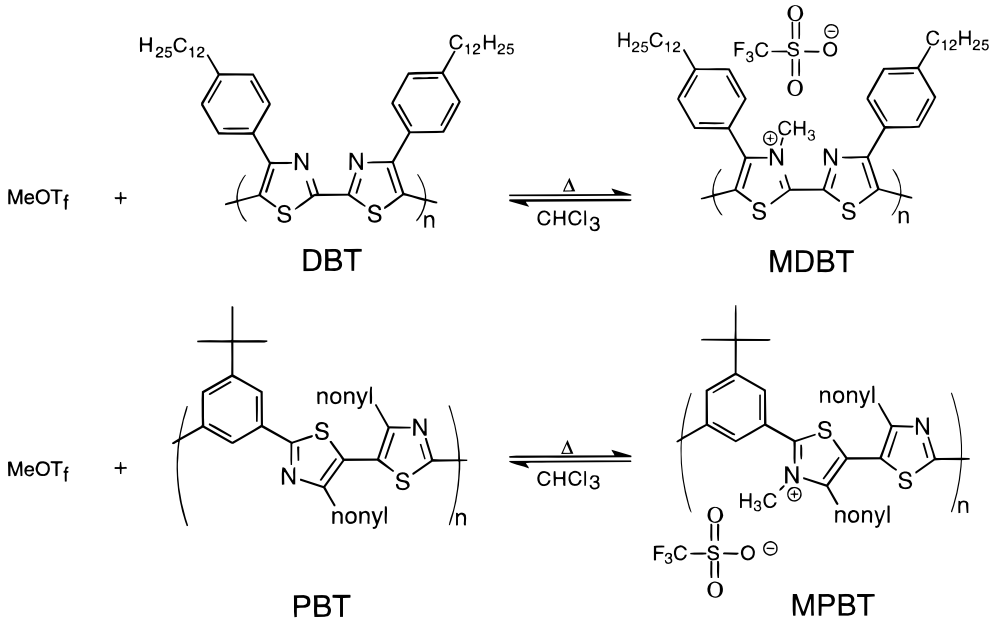

Table 1. Reaction Conditions for the Synthesis of MDBTs[a]

polym	MeOTf/N-atom[b]	time of reacn	temp[c]	% F
M-6-DBT	4	7 h	rt	0.70
M-8-DBT	7	30 h	rt	0.90
M-26-DBT	11	66 h	rt	3.00
M-40-DBT	6	2 days	50 °C	4.68
M-91-DBT[d]	7	7 days	50 °C	10.60
M-100-DBT[e]	7	7 days	50 °C	14.04

[a] An excess of methyltriflate was used in all cases. [b] The number of equivalents of methyltriflate used per N-atom. [c] rt = room temperature. [d] Synthesized from MDBT (100%) via Soxhlet extraction of excess methyltriflate with hexanes. [e] Flourine anaylsis indicates that excess methyltriflate is trapped in the polymer. This polymer was used as synthesized.

(50 mL) was added to try to dissolve the solid, but the solid did not dissolve. After 3 days, the solvent was removed and the brittle yellow solid was collected; yield = 0.76 g. ^{1}H NMR ($(CD_3)_2CO$): δ 0.84 (t, J = 3.6 Hz), 1.15−1.40 (m), 1.48 (s), 1.75−1.92 (unresolved m), 2.90−3.05 (unresolved m), 3.05−3.20 (unresolved m), 4.18 (s), 4.30 (s), 8.23−8.46 (aromatic protons). λ_{max}(abs) = 324 nm, 363 nm (film). λ_{max}(em) = 476 nm (film). FT-IR (KBr): ν_{NCS} = 1455 cm^{--1}, $\nu_{triflate}$ = 639, 1033, 1258 cm^{-1}. Fluorine analysis: 11.65% (85% *N*-methylation or 1.7 N−Me groups/bithiazole unit).

General Procedure for the Synthesis of Methylated Poly(4,4′-bis(*p*-dodecylphenyl)-2,2′-bithiazole-5,5′-diyl) (MDBT). A 100 mL Schlenk flask was charged with poly(4,4′-bis(*p*-dodecylphenyl)-2,2′-bithiazole-5,5′-diyl) (DBT)[17,21] (0.46 g, 0.71 mmol) in $CHCl_3$ (70 mL). Methyltriflate (1.45 g, 1 mL, 8.8 mmol) was added in two increments 24 h apart. The reaction mixture was heated at 50 °C for 2 days, and solvent was removed to give a red film; yield = 0.56 g. ^{1}H NMR ($CDCl_3$): δ 0.80−0.88 (br), 1.10−1.45 (m), 1.55−1.67 (br), 2.53−2.65 (br), 7.02−7.15 (br), 7.67−7.75 (br). λ_{max}(abs) = 456 nm (film). λ_{max}(em) = 568 nm (film). FT-IR (KBr): ν_{NCS} = 1455 cm^{--1}, $\nu_{triflate}$ = 646, 1033, 1258 cm^{-1} Fluorine analysis: 4.68% (40% *N*-methylation or 0.8 N−Me groups/bithiazole unit). Table 1 lists the times and temperatures used to obtain different percentages of *N*-methylation.

Results and Discussion

Preparation. Scheme 1 illustrates the reaction of methyltriflate with PBT and DBT to form the *N*-methylated derivatives, MDBT and MPBT, respectively. Due to an equilibrium that exists between the methylated and unmethylated polymers in solution, an excess of methyltriflate was used in all cases in order to drive the methylation reaction to completion. The extent of methylation was controlled by adjusting two variables: exposure time to methyltriflate and temperature. To obtain low degrees of methylation, relatively short exposure times, between 6 and 24 h, were used in combination with stirring at room temperature. Higher amounts of alkylation were attained through longer exposure times, 2−3 days, and with mild heating, up to 50 °C. In this way, a series of MDBTs were synthesized with differing amounts of methylation. This series of polymers was used to study the effect of varying the amount of *N*-methylation between 0 and 100% (every nitrogen quaternized). Table 1 summarizes the reaction conditions for the MDBTs.

The reagent, methyltriflate, was chosen to quaternize the ring N-atoms for two reasons. First, the nitrogen in the ring is a relatively weak nucleophile (pK_a = 1.0−3.0,[22−24] depending upon the ring substituents), and, consequently, a strong alkylating agent is required for the quaternization. Second, the triflate anion provides a good "handle" for determining the extent of methylation. The triflate anion contains the only fluorine in the polymer sample. Hence, fluorine analysis gives the concentration of the triflate ion, and since there is one triflate ion per quaternized N-atom, the extent of *N*-methylation is thereby determined. Also, the triflate ion has strong IR bands at ν = 1258, 1033, and 646 cm^{-1}, allowing further characterization of the extent of methylation by FT-IR analysis.

Figure 1 overlays the IR spectra of DBT with M-40-DBT and M-100-DBT (the number designates the percent of N-atoms that are methylated; e.g., M-40-DBT means that 40% of the N-atoms in DBT have been quaternized). As the extent of methylation increases, so does the concentration of the triflate counterion, and since *N*-methylation does not significantly alter the intensity of the ring mode at 1455 cm^{-1}, the intensities of the triflate peaks increase relative to those of the ring. These ratios may also be used to assess the extent of *N*-methylation.

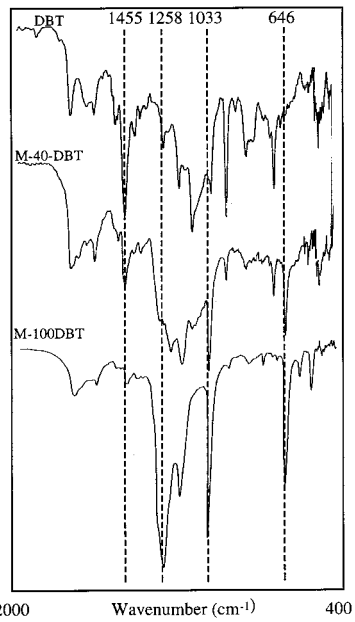

Figure 1. FT-IR spectra of DBT, M-40-DBT, and M-100-DBT.

Proton NMR proved to be ineffectual in characterizing the methylated polymers. The methylated polymers dissolve completely in $CHCl_3$ (MDBT) or acetone (MPBT), but, in solution, the triflate ion displaces the methyl group from the weakly basic N-atom, resulting in the equilibrium shown in Scheme 1 as indicated by the appearance of two peaks at 4.18 and 4.30 ppm due to methyltriflate and the *N*-methyl groups in the polymer, MPBT, respectively. In addition, the peak due to the *N*-methyl protons in the more rigid polymer, MDBT, is broadened to such an extent that it is essentially unobservable. This phenomenon has also been observed for the α-CH_2 protons in the NMR spectrum of poly(nonylbithiazole), and the effect was ascribed to a low tumbling rate of the groups directly attached to the rigid polymer backbone.[25] The low tumbling rate results in a "solid-like" spectrum characterized by broad peaks arising from dipole−dipole interactions and chemical shift anisotropy. However, the methylation of DBT was confirmed by both the presence of the triflate anion bands in the FT-IR spectrum and the detection of fluorine by chemical analysis.

Optical Properties. The UV−vis spectra of both PBT and DBT films red shift upon *N*-methylation. The red shifts are 50 nm, from 420 to 473 nm for M-100-DBT, and 26 nm, from 338 to 364 nm for M-85-PBT. Molecular orbital (MO) calculations for methylbithiazole show that this is an electronic effect that arises from the fact that both the HOMO and LUMO have electron density on the nitrogen atom. Thus, upon methylation, the formation of a positive charge on the nitrogen atom lowers the energy of both orbitals. However, because of the greater amount of electron density on the nitrogen in the LUMO; its energy is lowered more than that of the HOMO; therefore, the optical band gap decreases, resulting in the longer wavelength absorption. Figure 2 illustrates the changes in the energies of the HOMOs and LUMOs of methylbithiazole (MBT) and diprotonated MBT, MBT-H_2^{+2} calculated by the PM3 method in the CAChe MOPAC suite. Also shown are the representations of the HOMO and LUMO of MBT. The calculated band gaps are larger than the measured values, but the trends in energies are expected to be more reliable than their absolute values. Hence, these trends may be compared to those observed for the polymers DBT, M-100-DBT, PBT, and M-85-PBT which have band gaps of 2.65, 1.94, 2.94, and 2.81 eV, respectively. (Band gaps were measured by linearly extrapolating the low-energy side of the absorption band to zero absorption.) Unfortunately, the absolute values of the HOMO and LUMO energies with respect to the vacuum could not be established because a reliable reduction potential could not be measured for the heavily methylated polymers. The difficulty of measuring the reduction potential is related to the equilibrium shown in Scheme 1. In the polar solvent containing dissolved electrolyte (Bu_4NPF_6), displacement of the *N*-methyl group gave a mixture in which the degree of methylation is not known. This displacement reaction was evident by the reduction peaks attributable to methyltriflate, confirmed by the addition of methyltriflate to the analyte solution.

The greater shift in MDBT vs MPBT is caused by the difference in the effective conjugation length of the two polymers. DBT, with a longer effective conjugation length than PBT, has more methylation sites available, i.e., more nitrogens, per chromophore. Since the electronic effect of each quaternized nitrogen is additive, the shift in DBT is more dramatic.

Figure 3 is a plot of the UV−vis spectra of DBT and MDBT films. Overall, with increasing amounts of methylation, longer wavelength absorption was observed.

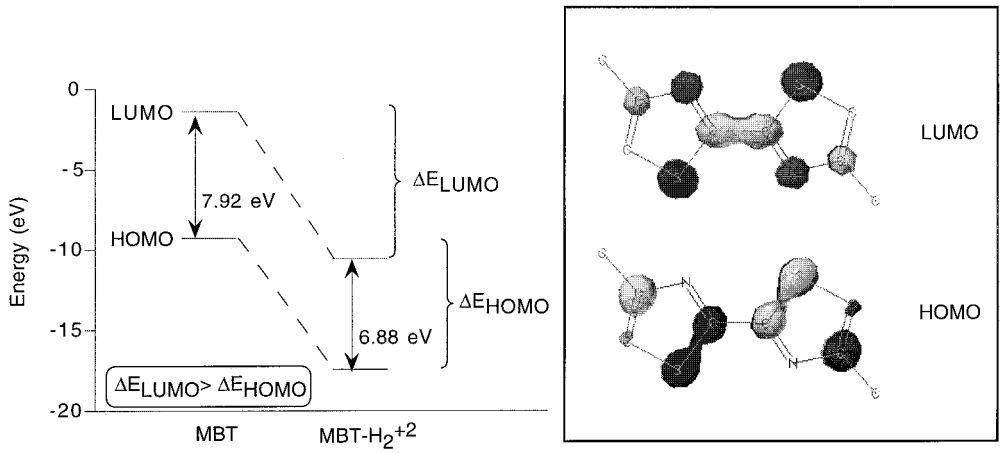

Figure 2. Calculated energy levels of the HOMOs and LUMOs for MBT and MBT-H_2^{2+} displayed with the extended Hückel calculated MOs of methylbithiazole.

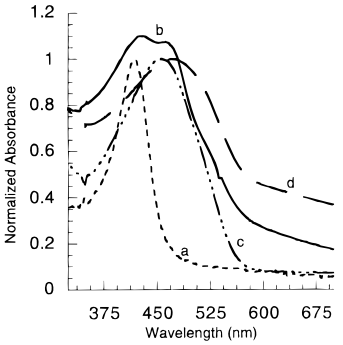

Figure 3. UV−vis spectra of DBT (a), M-26-DBT (b), M-40-DBT (c), and M-100-DBT (d) films.

The bimodal curve of M-26-DBT appears to result from a combination of two absorbing species: unmethylated and ∼50% methylated materials, as evidenced by the overlap of the peaks with those of DBT and M-40-DBT. As the percentage of alkylation was increased such that approximately every other nitrogen atom was alkylated, a single, broader absorbance peak at 456 nm appears (M-40-DBT). Finally, a maximum of 473 nm is reached with M-100-DBT. It should be noted that a red shifted absorbance was also observed when nonylbithiazole oligomers (NBT_n) were treated with either methyltriflate or triflic acid.[26]

The amount of the shift is determined by a combination of electronic and steric effects. In solution or in the solid state, the conjugated backbones of PBT and DBT are nonplanar due to steric repulsion between the large side chains. The steric repulsion twists the bithiazole rings out of coplanarity, leading to a shorter effective conjugation length and a blue shift of the λ_{max}. Since the observed spectra are seen to red shift with increasing *N*-alkylation, the electronic effect dominates the absorption (Figure 2). However, in the more planar poly(nonylbithiazole), a red shift, due to the electronic effect, is observed up to 50% methylation. With higher degrees of methylation, steric hindrance begins forcing the rings out of planarity causing a corresponding blue shift back to the λ_{max} of the original polymer.[27]

These spectral changes were modeled with calculations on protonated methylbithiazole. The absorption spectra of four compounds, planar methylbithiazole, planar, singly protonated methylbithiazole, planar, diprotonated methylbithiazole, and diprotonated methylbithiazole with a 90° torsion angle between the thiazole rings, were calculated with the MO program, Zindo. The predicted values for the absorption maxima were 356, 459, 533, and 418 nm, respectively. Thus, increasing the extent of protonation caused a red shift in the absorbance; however, when a twist between the thiazole rings, like that caused by stertic repulsion, was introduced, the absorbance blue shifted. These predictions are consistent with results of experiments in which the nitrogen atoms of 2,2′-bithiazole were bridged by alkyl chains of different lengths.[28] The shorter, C_2 chains keep the rings essentially coplanar, while the longer alkyl chains force the rings out of coplanarity. A blue shift in the absorbance was observed as the linkages were made longer. This steric vs electronic effect has also been observed in a bipyridinium system as well.[29]

The emission wavelengths of the polymer films also increase upon *N*-methylation. M-85-PBT emits at 478 nm, whereas PBT emits at 452 nm, a shift of 26 nm.

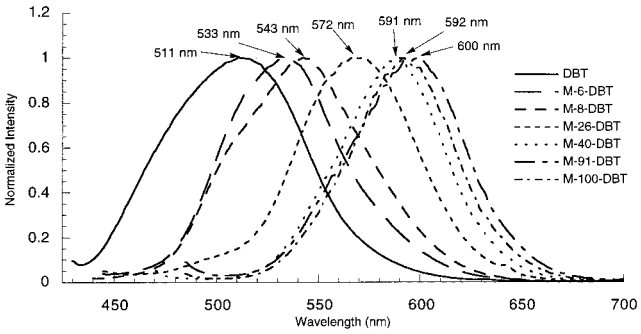

Figure 4. Emission spectra of DBT as a function of the extent of methylation.

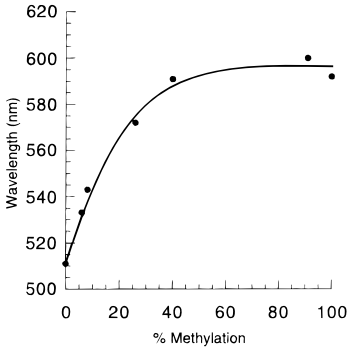

Figure 5. Plot of emission wavelength vs extent of methylation for MDBTs.

The corresponding emission wavelength for M-100-DBT and DBT are 593 and 511 nm, a shift of 82 nm. The larger shift in emission wavelength in DBT can be explained by its larger effective conjugation length as discussed above for the absorption spectra.

Quaternization of the N-atoms can be used to tune the emission wavelength through a range of colors. By varying the amount of alkylation, the emission color could be changed continuously from yellow to red. Figure 4 is a plot of the fluorescence spectra for films of MDBT with differing degrees of methylation. As with the UV−vis absorption spectra, increasing the extent of *N*-methylation shifts the emission to longer wavelengths, but the shifts level off at the higher degrees of methylation, as seen in Figure 5.

Electrochemistry. Methylation of the ring N-atoms is calculated to lower the energy levels of both the HOMO and LUMO. The reduction of a conjugated molecule occurs by placing an electron into the π^*-LUMO, while oxidation represents the removal of an electron from the π-HOMO. Lowering the energy level of the HOMO through alkylation increases the oxidation potential of the polymer, while lowering the energy level of the LUMO increases (makes more positive) the reduction potential.

Figure 6 is an overlay of the cathodic waves for DBT, M-26-DBT, and M-40-DBT. Increasing *N*-alkylation increases the reduction potential: DBT, −1.87 V; M-26-DBT, −1.61 V; and M-40-DBT (−1.31 V), a shift of 0.56 V with less than half the available N-atoms alkylated. An increased reduction potential was also observed for NBT oligomers.[26] The methylated polymers do not exhibit any oxidation within the range of the solvent system (range = −2 to +2 V) which is not surprising considering the already high oxidation potential of DBT, $E_{ox}^{p} = 1.05$ V.

Although the reduction potential increases with increasing alkylation, the upper limit of the reduction

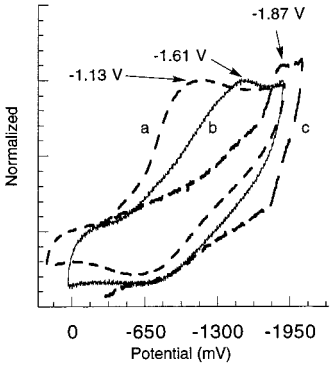

Figure 6. Cyclic voltammogram of DBT (c), M-26-DBT (b), and M-40-DBT (a) in a solution of 0.1 M $TBAPF_6$ in CH_2Cl_2 using a sweep rate of 200 mV/s (referenced vs Fc/Fc^+).

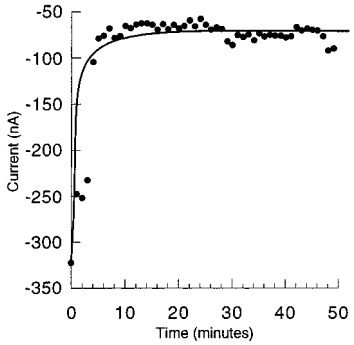

Figure 7. Plot of current vs time at −100 V for MPBT.

potential could not be obtained because the polar solvent and electrolyte shifts the equilibrium between methylated and unmethylated polymer as illustrated in eq 1.

$$R_3N\text{-}\overset{\oplus}{Me}\ \overset{\ominus}{O}Tf \rightleftharpoons R_3N + MeOTf \quad (1)$$

The solution CVs of the polymers with high degrees of methylation showed peaks due to free methyltriflate, while attempted CVs of the solid films were complicated by solubility of the methylated polymers and poor adhesion of the films to the electrode.

Conductivity. Since both MPBT and MDBT are polyelectrolytes, the conductivity is complicated by contributions of ionic conductivity to the electronic conductivity. The ionic conductivity comes from polarization and possible discharge of the ions, while the electronic portion arises from the transport of electrons through the π-system. Ionic conductivity can be eliminated by using DC current and ion-blocking electrodes and monitoring the current response over time at a constant potential until steady state is reached. Figure 7 shows a plot of current vs time at constant potential for MPBT. The initial, rapid change in the current is due to polarization of the mobile charges (ions) in the polymer matrix. However, after a short time, polarization is complete, and the "leftover" current is due solely to electronic conductivity. The difference between the final steady state and the initial current shows that 80% of the initial current was due to ionic polarization. Two probe conductivity measurements of each polymer film were performed, allowing enough time for polarization to occur and the current to stabilize, as shown in Figure 7. An increase of 8 and 6 orders of magnitude in the conductivity was observed in going from DBT to M-100-DBT and from PBT to M-85-PBT, respectively. Table 2 lists the conductivities of the different methylated

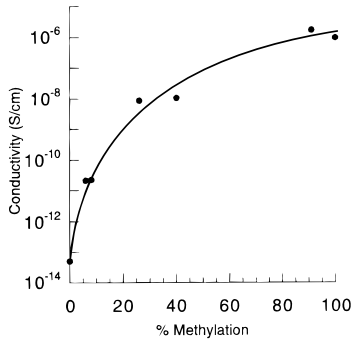

Figure 8. Plot of conductivity vs extent of methylation for MDBTs.

Table 2. Conductivity of the Polymers

polym	conductivity (S/cm)	polym	conductivity (S/cm)
DBT	5×10^{-14}	M-91-DBT	1×10^{-6}
M-6-DBT	2×10^{-11}	M-100-DBT	1×10^{-6}
M-8-DBT	2×10^{-11}	PBT	4×10^{-14}
M-26-DBT	9×10^{-9}	M-85-PBT	1×10^{-8}
M-40-DBT	1×10^{-8}		

polymers, and Figure 8 shows a plot of conductivity vs the extent of methylation for MDBTs.

The increase in conductivity upon methyation can be explained by three possible mechanisms. As conductivity is proportional to the number of charge carriers, one explanation could be that quaternization increases the number of charge carriers. Another explanation for the higher observed conductivity of the methylated polymers involves the increase in carrier mobility. The third explanation is simply a combination of the above.

Several methods for detecting charge carriers exist. One such method has been the use of near-IR spectra. "Free carriers" are known to absorb in the near IR, and in fact, this absorbance has been used to estimate the conductivity of a material.[21,30,31] The UV−vis−near-IR spectrum of MDBT shows a slight increase in the near-IR absorbance as compared to DBT. Unfortunately, the increase could not be resolved from possible baseline noise and therefore is inconclusive. The ESR spectra, further complicating matters, actually shows a decrease in the intensity of the $g = 2$ signal of M-40-DBT as compared to the DBT starting polymer. The diminished signal can be caused by either a spin pairing of the polarons[32] or by a decrease in the number of carriers. Again, these data are inconclusive.

Typically, in conducting polymers, increasing carrier mobility involves the extension of the conjugation length and the formation of π-stacks. However, in poly(nonylbithiazole), it has been observed that large amounts of methylation both shortens the effective conjugation length and disrupts the formation of π-stacks.[27] Hence, in order for the carrier mobility to increase, another mechanism must exist in this system. The comparison of the electron hopping mechanism of conductivity to an outer sphere electron-transfer redox reaction provides insight into a possible mechanism for increased carrier mobility.[33] The carrier mobility will be dependent upon a molecular reorganization energy as well as the energy associated with a counterion transfer.[34−36] It is difficult to predict how *N*-methylation would affect the reorganization energy; however, the counterion transfer should become easier in the methylated materials. In order for the electron to hop, the counterion must first bridge the two molecules and "condition" the receptor

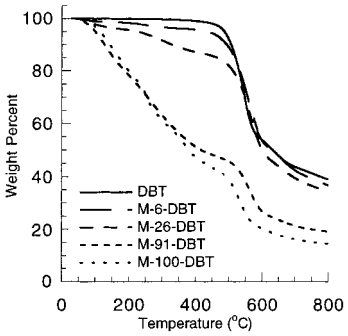

Figure 9. TGA traces of DBT overlaid with different MDBTs.

site for the transfer of the electron. In the methylated polymers, the concentration of counterions is larger, thus increasing the probability that a counterion will be adjacent to the receptor site. Hence, electron hopping can occur more readily in the "ionic atmosphere" of the *N*-methylated polymer, thereby increasing the carrier mobility. This theory also explains the leveling of the conductivity at higher degrees of methylation. After a certain amount of methylation, a critical concentration of counterion is reached such that the probability of ion exchange becomes essentially constant.

Thermal Stability. Both DBT and PBT exhibit high thermal stability: the 5% weight loss threshold occurs above 500 °C. Figure 9 shows the TGA curves of different MDBTs and of DBT. At lower temperatures, the percent weight loss is a function of the extent of *N*-methylation. As the samples are heated, the triflate ion attacks the *N*-methyl group, demethylation occurs, and the resultant methyltriflate is vaporized. The higher the degree of *N*-methylation, the greater is the weight percent of the overall polymer due to methyltriflate. Hence, a higher weight loss is observed for the polymers with the highest extent of methylation. However, it is apparent from the curves that the methylation does not effect the ring structure in that all of the traces show a sharp weight loss around 500 °C, which is similar to the original polymer, DBT. Although the percent weight loss prior to 500 °C parallels the percent *N*-methylation, it is difficult to pick out an inflection point that corresponds directly to the extent of methylation. It is important to note that the methylated polymers are shelf stable and that demethylation in the solid state is a function of temperature. The synthesis of these polymers included drying under vacuum (5 mTorr) at room temperature without significant loss of methyltriflate.

Light-Emitting Diodes. One potential use for these methylated polymers is as an electron transport/hole blocking (ETHB) layer in LEDs. Chemically, a good electron injection layer should have a high reduction potential (i.e. more positive) while a hole blocking layer should have a high oxidation potential. The higher conductivities of the methylated polymers compared to neutral conjugated systems also allows better electron transport. Fabrication of LEDs using the methylated polymers as the ETHB layer is underway. The results of these studies will be presented in a future paper.

Conclusions

The quaternization of bithiazole-containing polymers is a viable method of tuning various polymer characteristics. Both the optical properties and electrochemical properties were altered in a continuous manner upon *N*-methylation. The conductivity of these undoped polymers also increased up to 8 orders of magnitude with larger amounts of alkylation. A comparison of the effects of *N*-methylation on two polymers, MDBT and MPBT, shows that the effect of *N*-methylation is a function of the intrinsic properties of the polymer as well as the extent of methylation.

Acknowledgment. The authors thank the National Science Foundation (Grant DMR-9510274) for support for this research.

References and Notes

(1) Braun, D.; Heeger, A. J. *Appl. Phys. Lett.* **1991**, *58*, 1982.
(2) Burn, P. L.; Holmes, A. B.; Kraft, A.; Bradley, D. D. C.; Brown, A. R.; Friend, R. H. *J. Chem. Soc., Chem. Commun.* **1992**, 32.
(3) Grem, G.; Ledizky, G.; Ullrich, B.; Leising, G. *Adv. Mater.* **1992**, *4*, 36.
(4) Cimrova, V.; Remmers, M.; Neher, D.; Wegner, G. *Adv. Mater.* **1996**, *8*, 146.
(5) Horowitz, G. *Adv. Mater.* **1996**, *8*, 177.
(6) Dodabalapur, A.; Katz, H. E.; Torsi, L.; Haddon, R. C. *Science* **1995**, *269*, 1560.
(7) Lovinger, A. J.; Rothberg, L. J. *J. Mater. Res.* **1996**, *11*, 1581.
(8) McCullough, R. D.; Williams, S. P. *J. Am. Chem. Soc.* **1993**, *115*, 11608.
(9) McCullough, R. D.; Tristram-Nagle, S.; Williams, S. P.; Lowe, R. D.; Jayaraman, M. *J. Am. Chem. Soc.* **1993**, *115*, 4910.
(10) Conwell, E. *TRIP* **1997**, *5*, 218.
(11) Gill, R. E.; Hilberer, A.; van Hutten, P. F.; Berentschot, G.; Werts, M. P. L.; Meetsma, A.; Wittmann, J. C.; Hadziioannou, G. *Synth. Met.* **1997**, *84*, 637.
(12) Wu, M. W.; Conwell, E. M. *Phys. Rev. B* **1997**, *56*, R10060.
(13) Brazovskii, S.; Kirova, N.; Bishop, A. R.; Klimov, V.; McBranch, D.; Barashov, N. N.; Ferraris, J. P. *Opt. Mater.* **1998**, *9*, 472.
(14) Conwell, E. M. *Synth. Met.* **1997**, *85*, 995.
(15) Bunten, K. A.; Kakkar, A. K. *Macromolecules* **1996**, *29*, 2885.
(16) Wolf, M. O.; Wrighton, M. S. *Chem. Mater.* **1994**, *6*, 1526.
(17) Politis, J. K.; Nanos, J. I.; He, Y.; Kanicki, J.; Curtis, M. D. *Mater. Res. Soc. Bull* **1996**, *424*, 495.
(18) He, Y.; Politis, J. K.; Cheng, H.; Curtis, M. D.; Kanicki, J. *IEEE Trans. Electron Devices* **1997**, *44*, 1282.
(19) Politis, J. K.; Curtis, M. D. *Polym. Prepr.* **1997**, *38*, 379.
(20) Yamamoto, T.; Suganuma, H.; Maruyama, T.; Inoue, T.; Muramatsu, Y.; Arai, M.; Komarudin, D.; Ooba, N.; Tomaru, S.; Sasaki, S.; Kubota, K. *Chem. Mater.* **1997**, *9*, 1217.
(21) Politis, J. K.; Curtis, M. D.; Gonzalez, L.; Martin, D. C.; He, Y.; Kanicki, J. *Chem. Mater.* **1998**, *10*, 1713−1719.
(22) Barszcz, B.; Gabryszewski, M.; Kulig, J.; Lenarcik, B. *J. Chem. Soc., Dalton Trans.* **1986**, 2025.
(23) Alvarez-Ibarra, C.; Fernandez-Granda, R.; Quiroga, M. L.; Pingarron, J. M.; Pedrero, M. *Tetrahedron* **1996**, *52*, 11929.
(24) Moorthy, P. N.; Hayon, E. *J. Org. Chem.* **1977**, *42*, 879.
(25) Nanos, J. I.; Kampf, J. W.; Curtis, M. D.; Gonzalez, L.; Martin, D. C. *Chem. Mater.* **1995**, *7*, 2232.
(26) Curtis, M. D.; Nanos, J. I.; Cheng, H. T. Unpublished results.
(27) Curtis, M. D.; Cheng, H. T.; Johnson, J. A.; Nanos, J. I.; Kasim, R.; Elsenbaumer, R. L.; Gonzalez, L.; Martin, D. C. *Chem. Mater.* **1998**, *10*, 13.
(28) Goule, V.; Chirayil, S.; Thummel, R. P. *Tetrahedron Lett.* **1990**, *31*, 1539.
(29) Krumholz, P. *J. Am. Chem. Soc.* **1951**, *73*, 3487.
(30) Eliott, R. J.; Gibson, A. F. *An Introduction to Solid State Physics and Its Applications*; Macmillan Press: Basingstoke, U.K., 1974.
(31) Feldblum, A.; Kaufman, J. H.; Etemad, S.; Heeger, A. J. *Phys. Rev. B* **1982**, *26*, 815.
(32) Hill, M. G.; Penneau, J. F.; Zinger, B.; Mann, K. R.; Miller, L. L. *Chem. Mater.* **1992**, *4*, 1106.
(33) Cotton, F. A.; Wilkinson, G. *Advanced Inorganic Chemistry*; 5th ed.; John Wiley & Sons: New York, 1988.
(34) Blauch, D. N.; Saveant, J. M. *J. Am. Chem. Soc.* **1992**, *114*, 3323.
(35) Saveant, J. M. *J. Phys. Chem.* **1988**, *92*, 1011.
(36) Saveant, J. M. *J. Phys. Chem.* **1988**, *92*, 4526.

MA981242A